Journal of Engineering Research and Applied Science
Available at www.journaleras.com
Volume 10 (1), June 2021, pp 1689-1702
ISSN 2147-3471 © 2021

Geochemical features and petrogenesis of Late Cretaceous subduction-related volcanic rocks in the Değirmentaşı (Torul/Gümüşhane) area, Eastern Pontides (NE Turkey)

A. Kaygusuz[1,a], Ç. Saydam Eker[1]

[1]Gümüşhane University, Geological Engineering, Gümüşhane, Turkey.

Accepted 06 April 2021

Abstract
Mineralogical, petrographical and geochemical data are presented for the Late Cretaceous Değirmentaşı volcanics in the Eastern Pontides (NE Turkey). These volcanics are of sub-alkaline affinity and present features of subduction-related volcanism. K/Ar dating method carried out on hornblende of the Değirmentaşı volcanic rocks yielded 77.99±3.76 Ma, corresponding to the Campanian age. They are andesite, dacite and minor rhyolite in composition and consist of plagioclase, sanidine, quartz, biotite, hornblende and opaque minerals. The studied rocks show calc-alkaline affinities and have medium to high-K contents. The rocks are enriched in large-ion lithofile elements (LILEs) and light rare earth elements (LREEs) with pronounced depletion in high-field-strength elements (HFSEs) indicating the typical characteristics of rocks from the subduction-related tectonic setting. The chondrite-normalized REE patterns (LaN/LuN=4.5-13.8) have low to medium enrichment, demonstrating similar sources for the rock suite. The main solidification processes consist of fractional crystallization with minor amounts of crustal contamination. According to geochemical evidence, the parental magma(s) of the the Değirmentaşı volcanics rocks were possibly derived from a subcontinental lithospheric mantle enriched by fluids and/or sediments from a subduction of oceanic crust.

Keywords: late cretaceous, subduction, değirmentaşı volcanics, k-ar dating, geochemistry, eastern pontides.

1. Introduction

The Eastern Pontides, or also the eastern Sakarya Zone, generally contains Late Cretaceous volcanic and plutonic rocks that form widespread spreading in the region. The Eastern Pontides are represented by three main volcanic phases developed during Liassic, Late Cretaceous and Early Eocene to Miocene [1-2]. Although the Late Cretaceous aged plutons in the Eastern Pontides have been well studied in terms of their geochemical, isotopic and geochronological aspects [3-6]; the studies on their volcanic equivalents are limited [7-14]. The radiometric age data related to Late Cretaceous volcanics in Eastern Pontides are limited and are given in Table 1. The ages of the Late Cretaceous volcanics changes from 75 to 92 Ma (Table 1).

Studies on Late Cretaceous aged volcanic rocks in Torul region are limited [15-17]. Apart from the general geology of the study area [15, 18], there is no study on the petrology of the studied Late Cretaceous Değirmentaşı volcanics. In this study, new petrographic, geochemical, and K-Ar ages as well as field observations for the studied volcanic rocks are reported that enable to identify the magmatic evolution and the origin of this widespread subduction-related volcanic province in eastern Pontides.

2. Regional geology and stratigraphy

The Eastern Pontides orogenic belt is located within the Alpine–Himalayan orogenic belt. This belt is commonly subdivided into southern and northern zones, based on lithological and structural differences. The study area is located on the transition of northern-southern zone in the Eastern Pontides.

The basement rocks of the Eastern Pontides is represented by early Carboniferous metamorphic rocks [20] that are intruded by Middle-Late Carboniferous plutons [21-25]. These basement rocks

[a] Corresponding author; abdullah.kaygusuz@gmail.com

are unconformably overlain by the Jurassic volcanics, volcaniclastic and plutonic rocks [26-29]. The Jurassic rocks are conformably overlain by Late Jurassic-Early Cretaceous carbonate rocks [30]. The Late Cretaceous units that unconformably overlie these carbonate rocks consist of volcanic, plutonic and sedimentary rocks [10-11, 13-14, 31-32]. These rocks are overlain by Late Paleocene-Early Eocene adakitic rocks [33-34], Middle Eocene volcanic, sub-volcanic and sedimentary rocks [35-45] and cuts by Middle Eocene plutonic rocks [46-52]. These units are overlain by Neogene volcanic rocks [53] and are covered by Late Miocene and Plio–Quaternary adakitic volcanic-subvolcanic rocks [54]. Miocene and post-Miocene magmatisms are calc-alkaline to alkaline compositions in the Trabzon-Gümüşhane areas [53-54] and calc-alkaline in the Kandilli-Ilıca areas [55-56]. All units are unconformably overlain by Quaternary alluvium.

Table 1. Crystallization ages of Late Cretaceous volcanics in the Eastern Pontides

Name	Dating	Age (Ma)	Rock Types	Formation	Ref.
Değirmentaşı (Torul/Gümüşhane)	K-Ar	77.99±3.76	dacite	Kızılkaya	This study
Artvin	$^{206}Pb/^{238}U$	83.04±0.39	rhyolite	Kızılkaya	[13]
Artvin	$^{206}Pb/^{238}U$	86.51±0.35	rhyolite	Tirebolu	[13]
Murgul (Artvin)	$^{40}Ar/^{39}Ar$	92.1±1.2	basalt	Çatak	[12]
Murgul (Artvin)	$^{40}Ar/^{39}Ar$	88.8±0.9	dacite	Kızılkaya	[12]
Rize	$^{40}Ar/^{39}Ar$	83.2±1.0	dacite	Çayırbağ	[11]
Akçaabat (Trabzon)	$^{40}Ar/^{39}Ar$	82.61±0.34	basalt		[10]
Ordu	$^{206}Pb/^{238}U$	86.02±0.52	basalt		[9]
Ordu	$^{40}Ar/^{39}Ar$	75.34±0.10	rhyodacite		[9]
Tekke (Gümüşhane)	$^{206}Pb/^{238}U$	84.05±0.94	felsic tuff		[19]
Tekke (Gümüşhane)	$^{206}Pb/^{238}U$	81.09±0.62	felsic tuff		[19]
Tekke (Gümüşhane)	$^{206}Pb/^{238}U$	77.1±1.0	felsic tuff		[19]
Tirebolu (Giresun)	$^{206}Pb/^{238}U$	91.1 ± 1.3	dacite	Kızılkaya	[8]
Tirebolu (Giresun)	$^{208}Pb/^{232}Th$	83.1 ± 1.5	rhyolite	Çayırbağ	[8]
Maden (Bayburt)	$^{40}Ar/^{39}Ar$	80.9 ±0.9	trachyandesite		[7]
Zigana (Gümüşhane)	K-Ar	78.7 ± 2.3	dacite	Kızılkaya	[17]
Zigana (Gümüşhane)	K-Ar	75.3 ± 2.4	dacite	Kızılkaya	[17]
Hamsilos (Sinop)	$^{40}Ar/^{39}Ar$	79.0 ± 0.3	trachy basalt		[14]
Hamsilos (Sinop)	$^{40}Ar/^{39}Ar$	77.3 ± 0.4	trachy basalt		[14]
Hamsilos (Sinop)	$^{40}Ar/^{39}Ar$	78.2 ± 0.7	trachy basalt		[14]
Hamsilos (Sinop)	$^{40}Ar/^{39}Ar$	72.3 ± 0.5	basaltic andesite		[14]

Within the study area, the volcanic, plutonic and sedimentary rocks are observed (Figure 1). The oldest units in the study area are formed of neritic carbonates (Berdiga Formation; [30]). This unit unconformably overlain by andesite and their pyroclastics containing local limestone lenses (Çatak Formation [18]). These rocks are conformably overlain by the Late Cretaceous aged units consisting of dacite, rhyolite and pyroclastics (Kızılkaya Formation [18]). All these units are cut by Late Cretaceous aged intrusions [31-32].

Studied dasitic rocks exhibit well-developed columnar jointing. Large quartz grains can be selected macroscopically. Some of the dacite and rhyolites appear as domes. Pyroclastic rocks are composed of breccias, aglomerates and tuff, and are commonly interbedded with limestones.

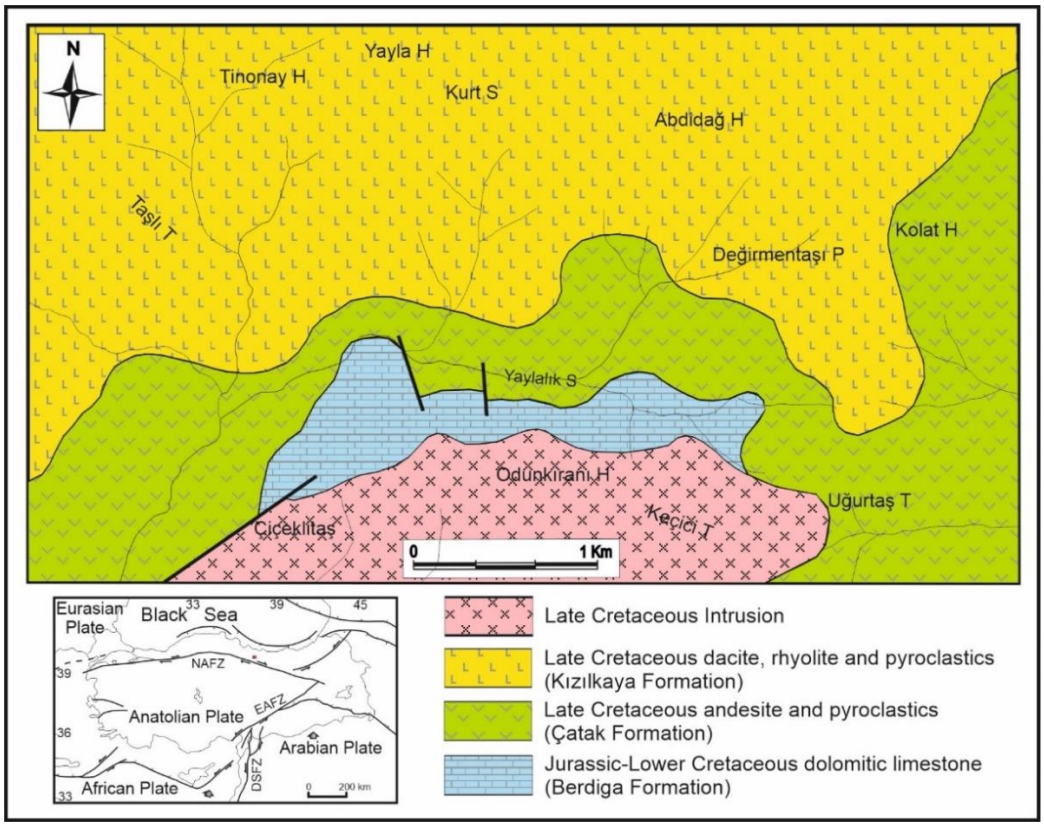

Figure 1. Geological map of the study area (modified by [15]).

3. Analytical procedures

In this study, 30 rock samples were collected from the Değirmentaşı (Torul/Gümüşhane) area. Based on microscopic studies, 11 of the freshest and most representative rock samples taken from lava flows were selected for whole-rock geochemical analysis.

Major and trace element including REE contents were performed at the ACME Laboratories Ltd. (Vancouver, Canada) using by ICP-emission spectrometry and ICP-mass spectrometry, using standard techniques. Major and trace elements were analyzed by ICP using 0.2 g of rock-powder fused with 1.5 g $LiBO_2$ and dissolved in 100 ml 5% HNO_3. REE analyses were performed by ICP-MS at ACME.

K-Ar isotopic analyses of the dacitic sample was determined at the Institute of Geology and Geophysics, Chinese Academy of Sciences (Beijing). Potassium (K) contents were examined using a spectrophotometer (type 6400) and two standards (trachyte ZGC and biotite ZBH-25) for callibration. The argon (Ar) contents were performed using a RGA10 massspectrometer and were adjusted to a trachyte standard ZGC and a biotite standard ZBH-25. The parameters used in the age calculation were: $\lambda = 5.543\times10\text{-}10/\text{year}$, $^{40}K/\Sigma K = 1.167\times10^{-4}$.

4. Results

4.1. Petrography

Based on their mineralogical, petrographical and textural characteristics, the studied volcanic rocks of the Değirmentaşı area are mainly andesites, dacites and minor rhyolites. Andesites have porphyritic, microlitic porphyritic and hyalo-microlitic porphyritic textures with phenocrystals consist of plagioclase, hornblende and biotite. Das have porphyritic texture including phenocrystals of plagioclase, quartz, sanidine and biotite. Rhyolites are porphyritic and partly spherulitic in texture. Phenocrystals are composed of plagioclase, sanidine, quartz, biotite and hornblend minerals. Opaque minerals, especially pyrites, are observed in all samples. The groundmass generally consists of feldspar microlites, Fe-Ti oxides and / or glass, sometimes alteration products (clay minerals, calcite, sericite, chlorite and epidote) and accessory apatite accompany them.

Plagioclases are widely observed in all samples as subhedral to euhedral phenocrystals and laths, and

microlites in the groundmass. They are mainly andesine ($An_{35–43}$) in andesites and andesine-oligoclase ($An_{25–36}$) in dacites and rhyolites. Plagioclase phenocrystals show albite and polysynthetic twinning, while small crystals show albite twinning. Oscillating zoning is observed in some minerals, while the others has sieve texture. Large plagioclases have poikilitic texture including small hornblende, opaque minerals and needle-like apatite inclusions. Some large crystals are partly sericitized and calcitized. Hornblendes are generally seen as euhedral to subhedral prismatic phenocrystals and microlites in the groundmass. Some crystals contain plagioclase and opaque mineral inclusions. They are occasionally chloritized and calcitized. Biotites are generally found in dacites and rhyolites as euhedral to subhedral crystals. Some biotite phenocrystals may contain small plagioclase and opaque minerals. Chloritization is common in some crystals. Quartz phenocrystals are commonly observed in dacites and rhyolites. They are partly corroded and skeletal. Embayed quartz crystals are common. Sanidine is generally seen as euhedral to subhedral lata-shaped crystals, and microcrystals in groundmass.

4.2. K–Ar geochronology

Following petrographical and geochemical evaluations, one sample freshly obtained from the Değirmentaşı volcanics were chosen for K–Ar analyses. K–Ar age determinations on the hornblende separates of one dacite sample is presented in Table 2. The sample yield age of 77.99 ± 3.76 Ma for the dasitic lava flow, corresponding to the Campanian (Late Cretaceous).

Table 2. K-Ar geochronologic data for the Değirmentaşı volcanics

Sample	Mineral	Age (Ma)	± σ	K (%)	^{40}Ar rad (%)	^{38}Ar (10^{-11}mol)	^{40}Ar/^{38}Ar	± σ	^{36}Ar/^{38}Ar	± σ
T62 (dacite)	Hb	77.99	3.76	0.32	25.17	2.20E-11	0.5319	0.00482	0.001373	0.0000177

λ= 5.543×10-10/year, ^{40}K/ΣK= 1.167×10-4, hb; hornblende

4.3. Whole-Rock Geochemistry

The whole-rock major and trace element (including REE) analyses for the rock samples from the Değirmentaşı volcanic rocks are listed in Table 3.

Table 3. Whole-rock major oxide (wt%), trace (ppm) and REE (ppm) analysis results of the Değirmentaşı volcanics.

Rock	andesite				dacite				rhyolite		
Sample	A9	M8	A10	T11	T62	H54	H3	T80	T113	H10	T102
SiO_2	58.27	59.06	59.85	62.92	69.00	69.18	69.64	69.71	69.54	71.10	71.87
TiO_2	0.48	0.60	0.37	0.38	0.31	0.39	0.43	0.32	0.28	0.35	0.22
Al_2O_3	16.17	16.25	16.89	16.46	14.56	17.44	15.78	14.49	14.26	14.94	13.34
$Fe_2O_3^T$	4.85	7.31	4.27	4.19	3.01	1.51	2.41	3.19	2.87	2.56	3.23
MnO	0.10	0.20	0.07	0.09	0.10	0.01	0.01	0.09	0.07	0.06	0.05
MgO	2.12	2.25	2.36	2.32	1.09	0.48	0.34	1.09	1.46	0.49	0.73
CaO	4.47	6.00	4.52	4.20	2.99	0.20	1.55	2.80	0.40	0.30	1.64
Na_2O	4.16	2.74	4.67	4.55	3.00	1.82	3.14	3.43	3.95	3.22	4.22
K_2O	1.18	1.41	1.57	1.03	3.33	4.45	2.47	2.96	4.25	4.25	2.19
P_2O_5	0.12	0.16	0.11	0.16	0.08	0.08	0.11	0.08	0.08	0.07	0.05
LOI	4.89	3.90	4.45	3.50	2.30	3.60	3.90	1.60	2.20	2.40	2.20
Total	96.81	99.88	99.13	99.80	99.77	99.16	99.78	99.76	99.36	99.74	99.74
Ni	46.0	4.1	30.0	6.6	1.3	0.5	0.6	1.1	1.0	1.8	0.7
V	182.0	173.0	96.0	72.0	52.0	17.0	56.0	52.0	42.0	42.0	22.0
Cu	38.0	61.6	45.0	1.8	1.1	2.7	3.1	2.3	2.1	1.1	0.4
Pb	46.0	3.1	52.0	63.0	48.3	7.8	4.7	31.1	30.1	7.1	20.4
Zn	67.0	74.0	88.0	36.0	22.0	18.0	29.0	34.0	41.0	47.0	13.0
W	0.5	0.7	0.8	0.7	0.9	3.6	3.0	1.3	1.3	2.5	0.7
Rb	36.0	28.4	48.0	22.2	63.9	152.1	68.6	67.0	96.3	111.6	37.9
Ba	513.0	567.9	627.0	214.0	1165.0	2502.0	1062.0	1017.0	1011.0	1720.0	1090.0
Sr	450.0	432.1	315.0	450.2	215.1	123.6	115.9	225.3	111.8	114.7	133.4
Ta	0.5	0.3	0.6	0.5	0.5	1.2	0.9	0.5	0.4	0.9	0.6

Nb	5.0	4.4	5.0	7.1	6.2	13.3	11.5	6.4	6.3	11.7	7.0
Hf	5.3	3.6	4.6	3.1	3.5	7.4	5.5	3.7	4.1	5.8	3.9
Zr	220.0	120.6	199.0	97.5	115.6	206.4	208.9	124.3	136.6	211.4	116.3
Y	28.0	22.6	21.0	14.9	18.5	20.7	26.0	20.9	17.7	23.9	22.7
Th	3.5	6.3	6.8	4.5	12.2	24.9	22.4	11.8	13.2	21.6	8.9
U	1.1	2.0	2.5	1.3	3.7	6.1	4.7	2.9	3.3	4.9	1.7
Ga	13.2	15.4	14.8	15.2	13.0	12.2	16.0	12.0	12.6	13.1	12.8
La	15.00	16.20	20.00	19.30	24.30	53.30	51.50	24.80	24.20	44.70	24.10
Ce	22.00	33.50	29.00	36.20	47.20	95.80	93.30	47.00	43.30	82.60	48.80
Pr	3.80	4.12	5.15	4.36	4.62	10.21	9.25	4.60	4.62	8.04	5.07
Nd	13.50	16.70	18.40	17.20	16.10	34.50	32.00	15.90	17.00	29.00	17.00
Sm	2.20	3.50	2.95	2.87	2.90	5.41	5.94	3.04	3.04	5.14	3.66
Eu	0.92	0.98	0.96	0.85	0.71	0.94	0.86	0.70	0.70	0.84	0.73
Gd	2.35	3.26	2.75	2.69	2.85	4.21	5.27	2.82	2.69	4.37	3.48
Tb	0.45	0.63	0.52	0.46	0.49	0.65	0.82	0.49	0.47	0.68	0.62
Dy	2.86	3.69	2.53	2.47	2.89	3.78	3.85	3.08	2.69	4.38	3.63
Ho	0.55	0.76	0.68	0.64	0.61	0.78	1.00	0.69	0.58	0.85	0.73
Er	1.45	2.36	1.86	1.79	2.00	2.17	2.81	2.01	1.86	2.65	2.41
Tm	0.26	0.37	0.24	0.21	0.27	0.37	0.42	0.32	0.28	0.41	0.37
Yb	1.76	2.36	1.82	1.70	1.96	2.44	3.03	2.21	1.97	2.67	2.42
Lu	0.26	0.37	0.28	0.24	0.31	0.40	0.44	0.35	0.31	0.44	0.38
$(La/Lu)_n$	5.97	4.53	7.40	8.33	8.12	13.80	12.12	7.34	8.08	10.52	6.57
$(Gd/Lu)_n$	1.12	1.09	1.22	1.39	1.14	1.31	1.49	1.00	1.08	1.23	1.14
$(Eu/Eu^*)_n$	1.23	0.87	1.01	0.92	0.75	0.58	0.46	0.72	0.73	0.53	0.62
Mg #	49.04	40.39	54.89	54.93	44.36	41.17	23.70	42.93	52.83	29.65	33.22
Mg# (mg-number) = molar 100xMgO/(MgO+ $Fe_2O_3^T$), LOI is loss on ignition, $Eu^*=(Sm+Gd)_{cn}/2$											

The studied volcanic rocks have SiO_2 contents from 58 to 72 wt.% (Table 3). The Mg numbers (Mg#) of the samples range from 24 to 55 (Table 2). K_2O/Na_2O ratios for the studied samples ranged from 0.2 to 2.5 (Table 3). In the classification diagram [57], the samples from the Değirmentaşı volcanics plotted in the andesite, dacite and minor rhyolite fields (Figure 2a). In the [58] classification diagram (Figure 2b), the rocks plot mainly in the andesite and dacite/rhyolite fields. The studied samples are sub-alkaline on the K_2O vs. SiO_2 diagram (Figure 2a) and are medium to high-K calc-alkaline in characters (Figure 3a). In the AFM triangle diagram [59], all of the samples are located in the calc-alkaline area, especially dacite and rhyolites show enrichment towards the alkaline end (Figure 3b).

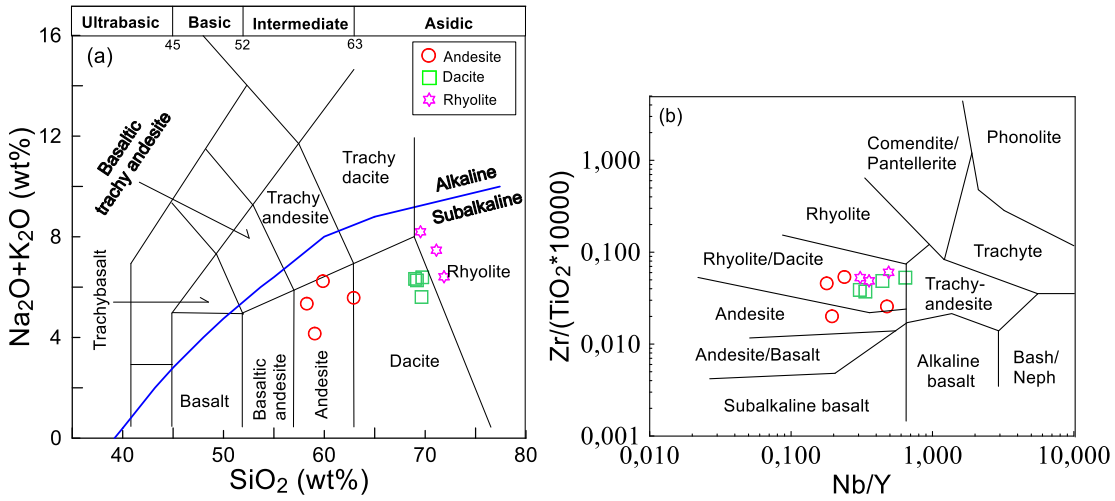

Figure 2. (a) Chemical classification diagram [57] and (b) SiO_2 vs. Zr/TiO_2 diagram [58] for the Değirmentaşı volcanic rocks (Alkaline-subalkaline dividing line is from [59]).

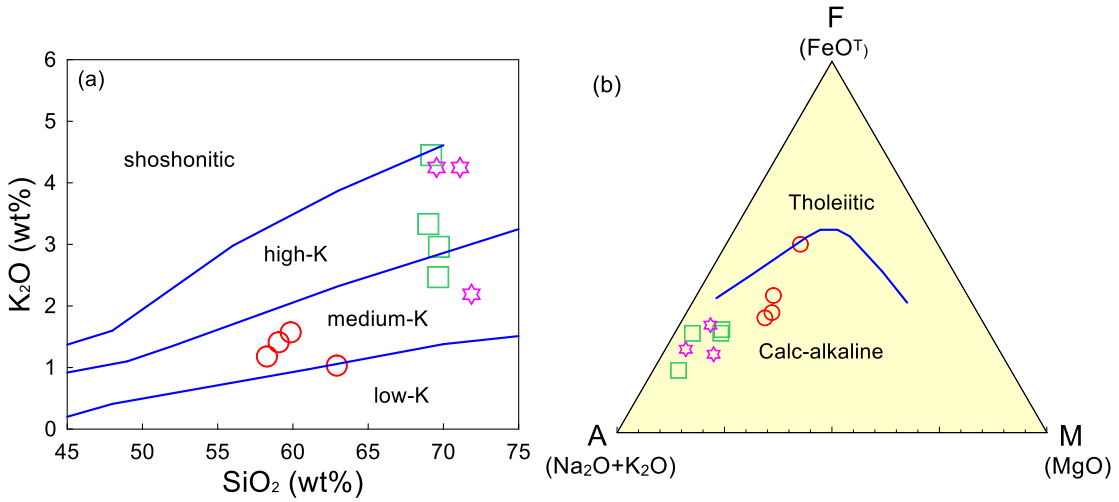

Figure 3. (a) SiO_2 vs. K_2O and (b) AFM [59] diagrams of the Değirmentaşı volcanic rocks. The field boundaries between medium-K, high-K and shoshonitic are from [60] (Alkaline–subalkaline and tholeiitic–calcalkaline dividing curves are from [59]).

Harker variations plots of the studied samples has systematic variations for some trace elements and major oxides (Figures 4 and 5). The MgO, CaO, $Fe_2O_{3(T)}$, Al_2O_3, P_2O_5, TiO_2, Sr, Zr, Y and Ni contents decrease, whereas K_2O, Th, Nb, Zr, Rb, Ba and La increase with increasing SiO_2 in the samples (Figure 4). The Na_2O and Pb show nearly constant trends (Figures 4 and 5).

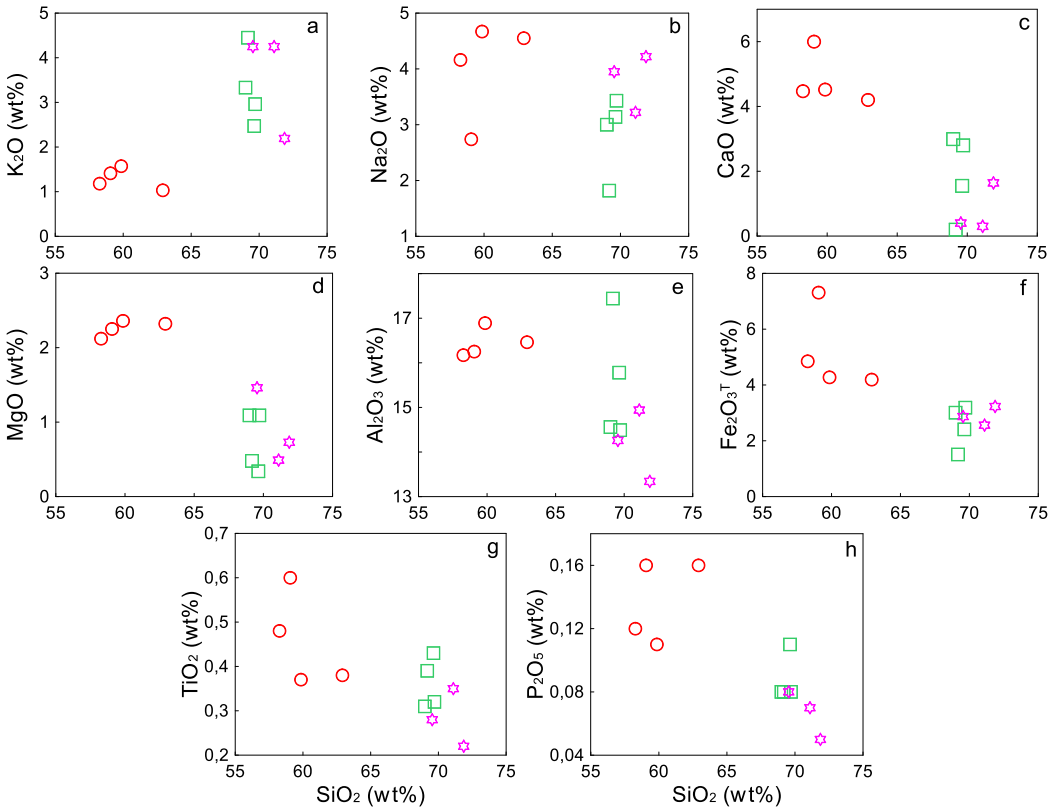

Figure 4. SiO_2 (wt%) versus major oxides (wt %) variation diagrams for samples from the Değirmentaşı volcanic rocks.

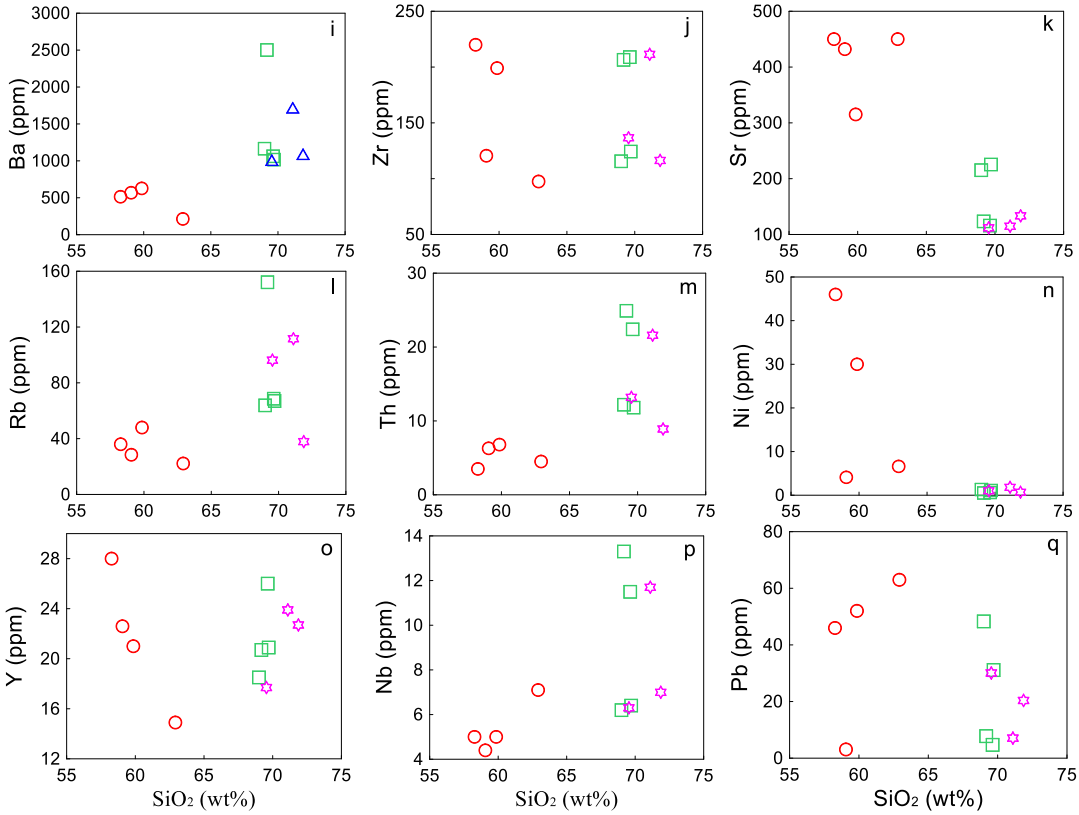

Figure 5. SiO_2 (wt%) vs. trace elements (ppm) variation diagrams for samples from the Değirmentaşı volcanic rocks

In primitive mantle-normalized spider diagrams, the studied samples display similar variations, and they are characterized by significant enrichment in LILEs, relative to some HFSEs, especially in Ti and P (Figures 6a and c). The samples have positive Pb anomalies. The enrichments in LILE elements along with the negative anomaly of Nb and Ta refers a subduction related magmatic processes and/or a crustal contamination [61] as seen in the studied samples. The chondrite-normalized REE for the samples have similar concave patterns with La_N/Lu_N= 4.53–13.80 (Table 3). These patterns are parallel to each other, showing a similar origin for the studied samples (Figures 6d and f). The heavy REE (HREE) profiles of all samples are almost flat (Gd_N/Lu_N = 0.99–1.49; Table 3). Basaltic samples have negativeto slightly positive Eu anomaly (Eu_N/Eu^*= 0.87–1.23; Table 3; Figure 6d). Dacitic and rhyolitic samples have negative Eu anomaly (Eu_N/Eu^*= 0.46–0.75; Table 3; Figures 6e and f).

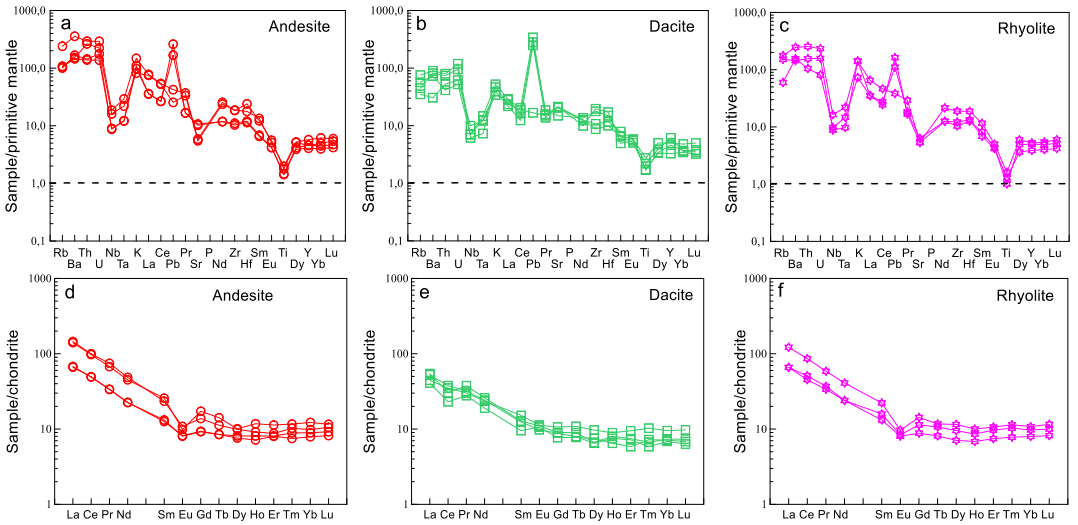

Figure 6. (a) Primitive mantle normalized (normalizing values from [62]) trace element patterns and (b) Chondrite normalized (normalizing values from [63]) trace element patterns for samples from the Değirmentaşı volcanic rocks

5. Discussion

5.1. Fractional crystallization (FC)

The Değirmentaşı volcanic rocks have similar geochemical and petrographical features and offer a typical K-rich calc-alkaline trend from andesites to rhyolites. They have similar LILE, HFSE, and REE patterns. In the selected major oxide and trace elements versus SiO_2 diagrams, observed well-defined negative or positive correlations with increasing silica (Figures 4 and 5) indicate that the fractional crystallization processes play important role during the evolution of the magmas of the Değirmentaşı volcanites. The rocks of the volcanics have high CaO and Sr contents and display weak negative Sr, Ba and Eu anomalies (Figures 8 and 9), which indicate fractionation of plagioclase. The decrease of Al_2O_3, $Fe_2O_3^T$, MgO, CaO and La contents and increase of K_2O and Ba values with increasing SiO_2 suggest calcic plagioclase and amphibole fractionation (Figures 4 and 5). The increases in K_2O and Rb with increasing SiO_2 content show that biotite and K-feldspar were not amongst the early phases of fractionation. The decrease in P_2O_5 and TiO_2 with increasing SiO_2 may results from removal of apatite and titanite during fractional crystallization, respectively (Figure 4).

The Y content of the samples exhibits a near-constant to positive correlation with increasing Rb contents (high-Y content, Figure 7a), which can be explained by clinopyroxene and plagioclase fractionation. In Rb/Sr vs. Sr (ppm) diagram (Figure 7b) show that the fractionation of plagioclase and hornblend played an important role in the evolution of the studied volcanic rocks.

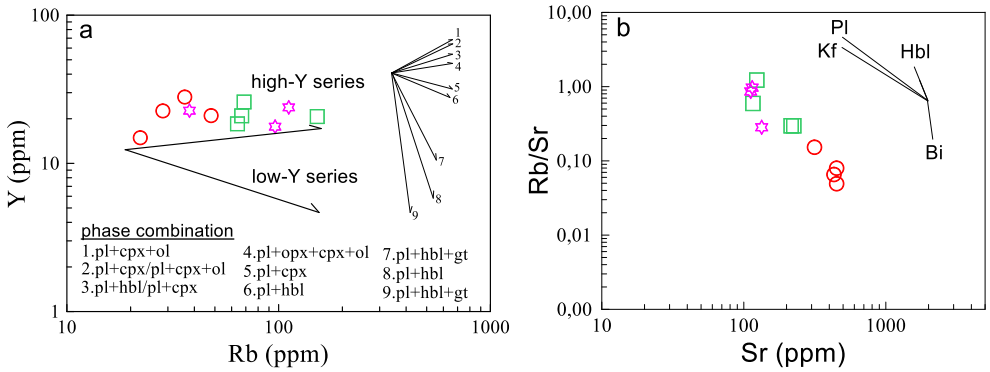

Figure 7. (a) Y vs. Rb and Rb/Sr vs. Sr diagrams for samples from the Değirmentaşı volcanic rocks. Fractionation trends are from [64].

5.2. Crustal contamination

In addition to fractional crystallization, crustal contamination can also be an important process during the evolution of magmatism in active continental margins. The continental crust is highly fractionated and enriched LREE with flat HREE and has negative Nb-Ta anomalies as well as positive Pb anomalies [63]. The Değirmentaşı volcanic rocks are characterized by pronounced positive Pb and negative Nb–Ta anomalies (Figure 5a), recording that subduction signature and possible minor amount of a crustal contribution in their evolution. Crustal components are also rich in Th (avg. 3.5 ppm) and Pb (avg. 8 ppm) in bulk continental crust [63]. Thus, the high Th (4 - 25 ppm) and Pb (3 - 63 ppm) values in the studied volcanic rocks may also be attributed to the effects of crustal contamination (Table 3).

5.3. Magma source

The Değirmentaşı volcanic rocks possess MgO values of 0.3–2.4%, Mg# values of 24–55 and Ni values of 1–46 ppm. These values indicate that Değirmentaşı volcanic rocks substantially differ from the magmas derived from primitive mantle composition (Mg# = ~ 66 to 75, Ni = ~ 400 to 500 ppm; [65]). The distribution pattern of the some major and trace elements of the studied samples (Figure 7a-i) support plagioclase ± amphibole + Fe-Ti oxide + apatite fractionations. Enrichments of LILEs and LREEs, and negative Ta and Nb anomalies (Figure 8a, b) together with low $(La/Yb)_N$ (4.6-14.8) ratios and high Th/Yb (2.0-10.2) ratios and Yb_N (6.9-12.2) values (Figure 6) of the studied samples indicate subduction-related metasomatised mantle source [66]. La/Sm vs. Ba/Th

and Th/Yb vs. Gd/Yb diagrams show that the melt was enriched in the fluids [67] during the Late Cretaceous subduction (Figure 8).

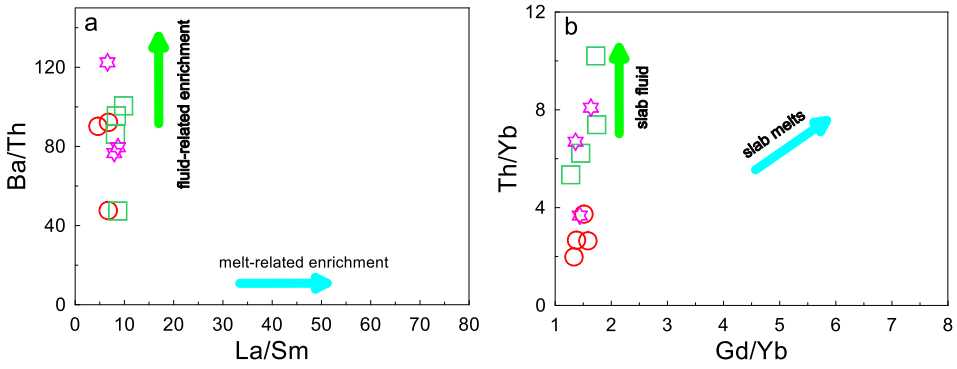

Figure 8. (a) Ba/Th vs. La/Sm and (b) Th/Yb vs. Gd/Yb diagrams for samples from the Değirmentaşı volcanic rocks.

In the Nb/Th vs. Nb diagram (Figure 9a) all samples plot in the arc volcanic sub-field. The low Ce/Pb ratios (0.3 to 19.9) of the studied samples are considerably different from those of oceanic basalts (~25 [68]), suggesting that these rocks are not derived from normal asthenospheric mantle. The Nb/Yb vs. Zr/Yb diagram (Figure 9b) indicates an apparent E-MORB composition. Low Sr/Y (4.5 to 30.2) and high Y (14.9 to 28.0 ppm) contents of the studied rocks imply that they are not adakitic rocks, and they show volcanic arc features (Figure 10a).

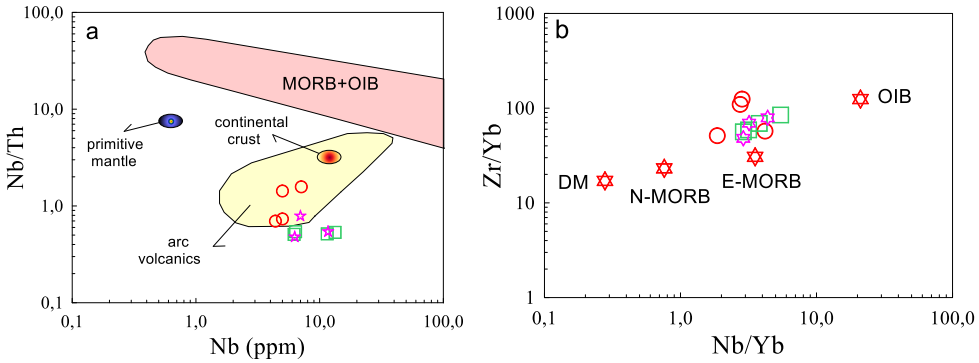

Figure 9. (a) Nb/Th vs. Nb and (b) Zr/Yb vs. Nb/Yb [61] diagrams from the Değirmentaşı volcanic rocks. For reference values in diagrams, see Figure 9 caption in [37].

[69] indicated that lower Nb/La ratios (~ < 0.5) suggest a lithospheric mantle source, whereas high Nb/La ratios (Nb/La > 1) demonstrate an OIB-like asthenospheric mantle source. The Nb/La (0.2–0.4) and La/Yb (6.9–21.8) ratios of the studied samples indicate a lithospheric mantle source (Figure 10b).

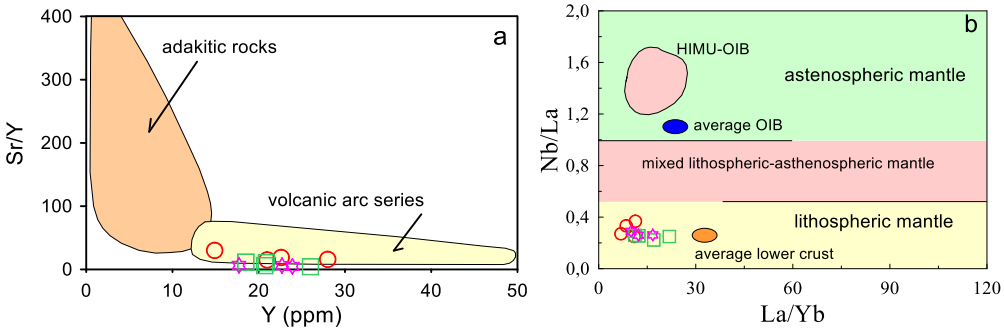

Figure 10. (a) Sr/Y vs. Y and (b) Nb/La vs. La/Yb diagrams from the Değirmentaşı volcanic rocks. For reference values in diagrams, see Figure 9 caption in [37].

In the Nb/Y vs. Th/Y diagram (Figure 11a), the Değirmentaşı volcanic rocks show a coherent trend, with a Th/Nb ratio close to 0.1, which may be attributed to the combined effects of fractional crystallisation and crustal assimilation. As shown in Figure 11, the displacement of this data array to higher Th/Y ratios compared to OIB and MORB can be considered strongly indicative of metasomatism of the mantle source by subduction zone fluids carrying the trace element signature of a crustal component. The Ta/Yb vs. Th/Yb diagram [64] can be used to identify the source variation and crustal contamination (Figure 11b). In Figure 11b, the studied volcanic rocks show a trend sub-parallel to the mantle array but shifted to higher Th/Yb ratios indicates melt derivation from a source enriched (or metasomatized) by fluids.

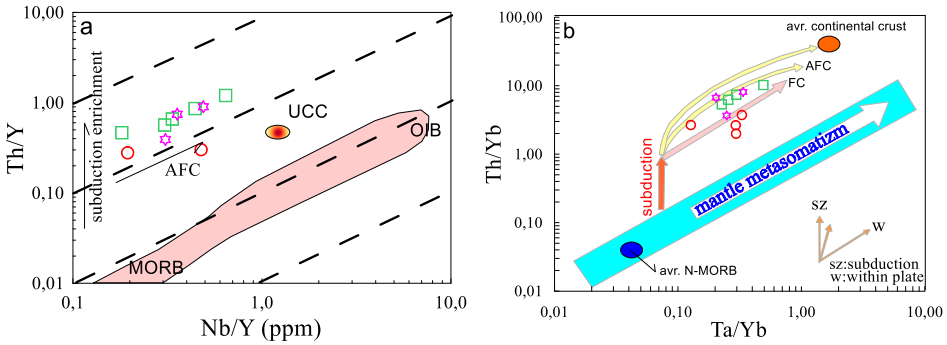

Figure 11. (a) Th/Y vs. Nb/Y and (b) Th/Yb vs. Ta/Yb [64] diagrams from the Değirmentaşı volcanic rocks. For reference values in diagrams, see Figure 9 caption in [37].

The Değirmentaşı volcanic rocks has relatively high and flat HREE patterns (Figure 6), indicating the absence of garnet in the mantle source region. Instead, these patterns are compatible with the presence of spinel in the mantle source. The negative Zr and P anomalies in the primitive mantle-normalized diagrams (Figure 6) could indicate the presence of residual zircon and apatite in the mantle source [70] or fractionation of these mineral phases during later petrogenetic processes. In addition, the relative HFSE depletion with respect to LILE can be explained by a mantle source modified via subduction-related fluids so that the LILEs are enriched. This may explain Ta, Nb, Zr and Ti depletion in the studied volcanics.

6. Conclusions

1. The studied Değirmentaşı volcanic rocks are andesite, dacite and minor rhyolite in composition defining a calc-alkaline series.
2. K-Ar dating on horblende separates from the lava flow gave an age of 77.99±3.76 Ma.
3. All the samples display similar geochemical features characterized by enrichment in large-ion lithofile elements and light rare earth elements, with pronounced depletion in high-field-strength elements indicating similar sources and petrogenetic processes.
4. The main solidification processes involved in the evolution of the studied volcanics consist of fractional crystallization with minor amounts of crustal contamination.
5. Plagioclase, hornblende and Fe-Ti oxides are the most important fractionating mineral phases.
6. The studied volcanic rocks were derived from a subcontinental lithospheric mantle enriched by fluids and/or sediments in a subduction-related geodynamic setting.

Acknowledgment

The author sincerely thanks Bin Chen during isotope analyses. Also thanks the editor and anonymous reviewer(s) for their improvement of the manuscript.

References

[1] Çamur, M.Z., Güven, T.B., Er, M. Geochemical characteristics of the Eastern Pontide volcanics: An example of multiple volcanic cycles in arc evolution, Turkish Journal of Earth Sciences 1996; 5: 123-144.

[2] Arslan, M., Tüysüz, N., Korkmaz, S. Kurt, H. Geochemistry and petrogenesis of the eastern Pontide volcanic rocks, Northeast Turkey, Chemie der Erde 1997; 57: 157-187.

[3] Kaygusuz, A., Arslan, M., Temizel, İ., Yücel, C., Aydınçakır, E., 2021. U–Pb zircon ages and petrogenesis of the Late Cretaceous I-type granitoids in arc setting, Eastern Pontides, NE Turkey, Journal of African Earth Sciences 2021; 174: 104040. doi.org/10.1016/j.jafrearsci.2020.104040.

[4] Karslı, O., Dokuz, A., Uysal, I., Aydin, F., Bin, C., Kandemir, R., Wijbrans, R.J. Relative contributions of crust and mantle to generation of Campanian high-K calc-alkaline I-type granitoids in a subdution setting, with special reference to the Harşit pluton, Eastern Turkey. Contributions to Mineralogy and Petrology 2010; 160: 467-487.

[5] Eyüboğlu, Y., Dudas, F.O., Zhu, D.C., Liu, Z., Chatterjee, N. Late Cretaceous Iand A-type magmas in eastern Turkey: Magmatic response to double-sided subduction of Paleo- and Neo-Tethyan lithospheres, Lithos 2019; 326-327: 39-70.

[6] Temizel, İ., Arslan, M., Yücel, C., Abdioğlu Yazar, E., Kaygusuz, A., Aslan, Z. U-Pb geochronology, bulk-rock geochemistry and petrology of Late Cretaceous syenitic plutons in the Gölköy (Ordu) area (NE Turkey): Implications for magma generation in a continental arc extension triggered by slab roll-back, Journal of Asian Earth Sciences 2019; 171: 305-320.

[7] Eyüboğlu, Y. Late Cretaceous high-K volcanism in the eastern Pontides orogenic belt, and its implications for the geodynamic evolution of NE Turkey, Int Geol Rev 2010; 52 (2-3): 142-186.

[8] Eyüboğlu, Y., Santosh, M., Yi, K., Tuysuz, N., Korkmaz, S., Akaryali, E., Dudas, F.O., Bektas, O. The Eastern Black Sea-type Volcanogenic Massive Sulfide Deposits: Geochemistry, zircon U-Pb geochronology and an overview of the geodynamics of ore genesis. Ore Geol Rev 2014; 59: 29-54.

[9] Özdamar, Ş. Geochemistry and geochronology of late Mesozoic volcanic rocks in the northern part of the Eastern Pontide Orogenic Belt (NE Turkey): Implications for the Closure of the Neotethys Ocean, Lithos 2016; 248-251: 240-256.

[10] Yücel, C. Akçaabat (Trabzon) Güneyi ve Çevresindeki Kampaniyen Yaşlı Volkanik Kayaçların Petrografisi, Jeokimyası, Jeokronolojisi ve Petrojenezi, Gümüşhane Üniversitesi, Fen Bilimleri Enstitüsü Dergisi 2017; 7 (1): 79-101.

[11] Alan, İ., Balcı, V., Keskin, H., Altun, İ., Böke, N., Demirbağ, H., Arman, S., Elibol, H., Soyakıl, M., Kop, A., Hanilçi, N. Tectonostratigraphic characteristics of the area between Çayeli (Rize) and İspir (Erzurum), Bulletin of the Mineral Research and Exploration 2019; 158: 1-29.

[12] Kandemir, Ö., Akbayram, K., Çobankaya, M., Kanar, F., Pehlivan, Ş., Tok, T., Hakyemez, A., Ekmekçi, E., Danacı, F., Temiz, U. From arc evolution to arccontinent collision: Late Cretaceous–middle Eocene geology of the Eastern Pontides, northeastern Turkey. Geological Society of America Bulletin 2019; 131 (11/12): 1889-1906.

[13] Aydın, F., Saka, S.O., Şen, C., Dokuz, A., Aiglsperger, T., Uysal, İ., Kandemir, R., Karslı, O., Sarı, B., Başer, R., Temporal, geochemical and geodynamic evolution of the Late Cretaceous subduction zone volcanism in the eastern Sakarya Zone, NE Turkey: implications for mantle-crust interaction in an arc setting, Journal of Asian Earth Sciences 2020; 192, 104217. https://doi.org/10.1016/j.jseaes.2019.104217.

[14] Aydınçakır, E. 2016. Subduction-related Late Cretaceous high-K volcanism in the Central Pontides orogenic belt: Constraints on geodynamic implications, Geodinamica Acta 28(4), 379-411.

[15] Kaygusuz, A. Torul ve çevresinde yüzeylenen kayaçların petrografik ve jeokimyasal incelenmesi. PhD Thesis, KTÜ-Trabzon 2000; 23 pp.

[16] Kaygusuz, A., Şen, C., Aslan, Z. Torul (Gümüşhane) Volkaniklerinin Petrografik ve Petrolojik Özellikleri (KD Türkiye); Fraksiyonel Kristallenme ve Magma Karışımına İlişkin Bulgular, Türkiye Jeoloji Bülteni 2006; 49, 1: 49-82.

[17] Sipahi, F. Zigana Dağı (Torul–Gümüşhane) volkanitlerindeki hidrotermal ayrışmaların mineraloji ve jeokimyası, PhD thesis, KTÜ Fen Bilimleri Enstitüsü, Trabzon; 2005.

[18] Güven, İ.H. 1:25000-Scale Geological and

Metallogenical Map of the Eastern Black Sea Region (in Turkish); Mineral Research and Exploration Institute of Turkey (MTA) Publications, Ankara, Turkey 1993; 98 pp.

[19] Eyuboğlu, Y. Petrogenesis and U–Pb zircon chronology of felsic tuffs interbedded with turbidites (Eastern Pontides Orogenic Belt, NE Turkey): implications for Mesozoic geodynamic evolution of the eastern Mediterranean region and accumulation rates of turbidite sequences. Lithos 2015; 212–215: 74-92.

[20] Topuz, G., Altherr, R., Kalt, A., Satır, M., Wemer, O., Schwarz, W.H. Aluminous granulites from the Pulur complex, NE Turkey: A case of partial melting, efficient melt extraction and crystallization, Lithos 2004; 72: 183-207.

[21] Topuz, G., Altherr, R., Wolfgang, S., Schwarz, W.H., Zack, T., Hasanözbek, A., Mathias, B., Satır, M., Şen, C. Carboniferous high-potassium I-type granitoid magmatism in the Eastern Pontides: The Gümüşhane Pluton (NE Turkey), Lithos 2010; 116: 92110.

[22] Kaygusuz, A., Arslan, M., Siebel, W., Sipahi, F., İlbeyli, N. Geochronological evidence and tectonic significance of Carboniferous magmatism in the southwest Trabzon area, eastern Pontides, Turkey. International Geology Rew 2012; 54 (15): 1776-1800.

[23] Kaygusuz, A., Arslan, M., Sipahi, F., Temizel, İ. U–Pb zircon chronology and petrogenesis of Carboniferous plutons in the northern part of the Eastern Pontides, NE Turkey: Constraints for Paleozoic magmatism and geodynamic evolution. Gondwana Research 2016; 39: 327-346.

[24] Vural, A., Kaygusuz, A. Petrology of the paleozoic plutons in Eastern pontides: artabel pluton (Gümüşhane, NE Turkey). Journal of Engineering Research and Applied Science 2019; 8 (2): 1216-1228.

[25] Kaygusuz, A. Geochronological age relationships of Carboniferous Plutons in the Eastern Pontides (NE Turkey). Journal of Engineering Research and Applied Science 2020; 9 (1): 1299-1307.

[26] Akaryalı, E., Akbulut, K. Constraints of C–O–S isotope compositions and the origin of the Ünlüpınar volcanic-hosted epithermal Pb–Zn ± Au deposit, Gümüshane, NE Turkey Journal of Asian Earth Science 2016; 117: 119-134.

[27] Aydınçakır, E., Gündüz, R., Yücel, C. Emplacement conditions of magma(s) forming Jurassic plutonic rocks in Gümüşhane (Eastern Pontides, Turkey). Bulletin of the Mineral Research and Exploration 2020; 162: 175–196.

[28] Dokuz, A., Karslı, O., Chen, B., Uysal, İ. Sources and petrogenesis of Jurassic granitoids in the Yusufeli area, northeastern Turkey: implications for pre- and post-collisional lithospheric thinning of the Eastern Pontides. Tectonophysics 2010; 480: 259-279.

[29] Saydam Eker, Ç., Sipahi, F., Kaygusuz, A. Trace and rare earth elements as indicators of provenance and depositional environments of Lias cherts in Gumushane, NE Turkey. Chemie der Erde Geochemistry 2012; 72: 167-177.

[30] Pelin, S. Geological study of the area southeast of Alucra (Giresun) with special reference to its petroleum potential. Karadeniz Teknik Üniversitesi Yayın No. 87, Trabzon 1977; 103 pp.

[31] Kaygusuz, A., Siebel, W., Şen, C., Satır, M. Petrochemistry and petrology of I-type granitoids in an arc setting: The Composite Bayburt Pluton, Eastern Pontides, NE Turkey. International Journal of Earth Sciences 2008; 97: 739-764.

[32] Kaygusuz, A., Siebel, W., İlbeyli, N., Arslan, M., Satır, M., Şen, C. Insight into magma genesis at convergent plate margins. A case study from the eastern Pontides (NE Turkey). Neues Jahrbuch Für Mineralogie 2010; 187/3: 265–287.

[33] Eyuboğlu, Y., Dudas, F.O., Santosh, M., Yi, K., Kwon, S., Akaryali, E. Petrogenesis and U-Pb zircon chronology of adakitic porphyries within the Kop ultramafic massif (Eastern Pontides Orogenic Belt, NE Turkey). Gondwana Research 2013; 24 (2): 742–766.

[34] Topuz, G., Okay, AI., Altherr, R., Schwarz, WH., Siebel, W., Zack, T., Satır, M., Şen, C. Post-collisional adakite-like magmatism in the Ağvanis Massif and implications for the evolution of the Eocene magmatism in the Eastern Pontides (NE Turkey). Lithos 2011; 125: 131–150.

[35] Tokel, S. Doğu Karadeniz Bölgesi'nde Eosen yaşlı kalk-alkalen andezit1er ve jeotektonizma, TJK Bülteni 1977; 20/1: 49-54.

[36] Aslan, Z., Arslan, M., Temizel, İ., Kaygusuz, A. K-Ar dating, whole-rock and Sr-Nd isotope geochemistry of calc-alkaline volcanic rocks around the Gümüşhane area: implications for post-collisional volcanism in the Eastern Pontides, Northeast Turkey. Mineralogy and Petrology 2014; 108: 254-267.

[37] Kaygusuz, A., Arslan, M., Siebel, W., Şen, C. Geochemical and Sr-Nd isotopic characteristics

of post-collisional calc-alkaline volcanics in the Eastern Pontides (NE Turkey) Turkish Journal of Earth Sciences 2011; 20: 137-159.

[38] Kaygusuz, A., Merdan Tutar, Z., Yücel, C. Mineral chemistry, crystallization conditions and petrography of Cenozoic volcanic rocks in the Bahçecik (Torul/Gümüşhane) area, Eastern Pontides (NE Turkey). Journal of Engineering Research and Applied Science 2017; 6 (2): 641-651.

[39] Temizel, İ., Arslan, M., Ruffet, G., Peucat, J.J. Petrochemistry, geochronology and Sr-Nd ısotopic systematic of the Tertiary collisional and postcollisional volcanic rocks from the Ulubey (Ordu) area, Eastern Pontide, NE Turkey: Implications for extension-related origin and mantle source characteristics, Lithos 2012; 128: 126-147.

[40] Arslan, M., Temizel, İ., Abdioğlu, E., Kolaylı, H., Yücel, C., Boztuğ, D., Şen, C. 40Ar-39Ar dating, whole-rock and Sr-Nd-Pb isotope geochemistry of post-collisional Eocene volcanic rocks in the southern part of the Eastern Pontides (NE Turkey): Implications for magma evolution in extension-ınduced origin, Contributions to Mineralogy and Petrology 2013; 166: 113-142.

[41] Yücel, C., Arslan, M., Temizel, İ., Abdioğlu Yazar, E., Ruffet, G. Evolution of K-rich magmas derived from a net veined lithospheric mantle in an ongoing extensional setting: Geochronology and geochemistry of Eocene and Miocene volcanic rocks from Eastern Pontides (Turkey). Gondwana Research 2017; 45: 65-86.

[42] Kaygusuz, A., Şahin, K. Petrographical, geochemical and petrological characteristics of Eocene volcanic rocks in the Mescitli area, Eastern Pontides (NE Turkey), Journal of Engineering Research and Applied Science 2016; 5 (2): 473-486.

[43] Kaygusuz, A., Selvi, D. Crystallization conditions and petrography of eocene volcanic rocks in the Gümüşdamla-Erikdibi area (Bayburt, NE Turkey). Journal of Engineering Research and Applied Science 2020; 9 (2): 1529-1537.

[44] Kaygusuz, A., Gücer, M.A., Yücel, C., Aydınçakır, E., Sipahi, F. Petrography and crystallization conditions of Middle Eocene volcanic rocks in the Aydıntepe-Yazyurdu (Bayburt) area, Eastern Pontides (NE Turkey). Journal of Engineering Research and Applied Science 2019; 8 (2): 1205-1215.

[45] Saydam Eker, Ç. Petrography and Geochemistry of Eocene Sandstones from Eastern Pontides (NE Turkey): Implications for Source Area Weathering, Provenance and Tectonic Setting, Geochemistry International 2012; 50 (8): 683–701.

[46] Karslı, O., Chen, B., Aydın, F., Şen, C. Geochemical and Sr-Nd-Pb ısotopic compositions of the Eocene Dölek and Sarıçiçek Plutons, Eastern Turkey: Implications for magma ınteraction in the genesis of high-K calc-alkaline granitoids in a post-collision extensional setting, Lithos 2007; 98: 67-96.

[47] Temizel, İ., Abdioğlu Yazar, E., Arslan, M., Kaygusuz, A., Aslan, Z. Mineral chemistry, whole-rock geochemistry and petrology of Eocene I-type Shoshonitic plutons in the Gölköy area (Ordu, NE Turkey), Bulletin of the Mineral Research and Exploration 2018; 157: 121-152.

[48] Temizel, İ., Arslan, M., Yücel, C., Abdioğlu Yazar, E., Kaygusuz, A., Aslan, Z. Eocene tonalite–granodiorite from the Havza (Samsun) area, northern Turkey: Adakite-like melts of lithospheric mantle and crust generated in a post-collisional setting. International Geology Review 2020; 62 (9): 1131-1158.

[49] Kaygusuz, A., Öztürk, M. Geochronology, geochemistry, and petrogenesis of the Eocene Bayburt intrusions, Eastern Pontide, NE Turkey: implications for lithospheric mantle and lower crustal sources in the high-K calc-alkaline magmatism. Journal of Asian Earth Sciences 2015; 108: 97-116.

[50] Vural, A., Kaygusuz, A. Geochronology, petrogenesis and tectonic importance of Eocene I-type magmatism in the Eastern Pontides, NE Turkey. Arabian Journal of Geosciences 2021; 14: 467. doi.org/10.1007/s12517-021-06884-z.

[51] Kaygusuz, A., Yücel, C., Arslan, M., Sipahi, F., Temizel, İ., Çakmak, G., Güloğlu, Z.S. Petrography, mineral chemistry and crystallization conditions of Cenozoic plutonic rocks located to the north of Bayburt (Eastern Pontides, Turkey), Bulletin of the Mineral Research and Exploration 2018; 157: 75-102.

[52] Kaygusuz, A., Yücel, C., Arslan, M., Temizel, İ., Yi, K., Jeong, Y-J., Siebel, W., Sipahi, F. Eocene I-type magmatism in the Eastern Pontides, NE Turkey: Insights into magma genesis and magma-tectonic evolution from whole-rock geochemistry, geochronology and isotope systematics, International Geology Review 2020; 62 (11): 1406-1432.

[53] Aydın, F., Karslı, O., Chen, B. Petrogenesis of the Neogene alkaline volcanics with

ımplcations for post collisional lithospheric thinning of the Eastern Pontides, NE Turkey, Lithos 2008; 104: 249-266.

[54] Yücel, C. Geochronology, geochemistry, and petrology of adakitic Pliocene–Quaternary volcanism in the Şebinkarahisar (Giresun) area, NE Turkey. International Geology Review 2019; 61, 6: 754-777.

[55] Kaygusuz, A. K/Ar ages and geochemistry of the post-collisional volcanic rocks in the Ilıca (Erzurum) area, eastern Turkey. Neues Jahrbuch Für Mineralogie 2009; 186/1: 21-36.

[56] Kaygusuz, A., Aslan, Z., Aydınçakır, E., Yücel, C., Gücer, M.A., Şen, C. Geochemical and Sr-Nd-Pb isotope characteristics of the Miocene to Pliocene volcanic rocks from the Kandilli (Erzurum) area, Eastern Anatolia (Turkey): Implications for magma evolution in extension-related origin. Lithos 2018; 296/299: 332-351.

[57] Le Maitre, R.W., Bateman, P., Dudek, A., Keller, J., Lameyre Le Bas, M.J., Sabine, P.A., Schmid, R., Sorensen, H., Streckeisen, A., Woolley, A.R., Zanettin, B.A Classification of ıgneous rocks and glossary of terms, Blackwell, 1989; Oxford.

[58] Winchester, J.A., Floyd, P.A. Geochemical discrimination of different magma series and their differentiation products using immobile elements. Chemical Geology 1977; 20: 325-343.

[59] Irvine, T.N., Baragar, W.R.A. A guide to the chemical c1assification of common volcanic rocks, Canadian Journal of Earth Sciences 1971; 8: 523-548.

[60] Peccerıllo, R., Taylor, S.R. Geochemistry of Eocene calcalkaline volcanic rocks from the Kastamonu area, northern Turkey. Contributions to Mineralogy and Petrology 1976; 58: 63-81.

[61] Pearce, J.A., Peate, D.W. Tectonic implications of the composition of volcanic arc magmas. Annual Review of Earth and Planetary Science Letters 1995; 23: 251-285.

[62] Sun, S., McDonough, W.F. Chemical and ısotopic systematics of oceanic basalt: Implications for mantle composition and processes, In: A. D. Saunders, ve M.J. Norry, (eds.), Magmatism in the Ocean Basins, Geological Society of London, Special Publication 1989; 42: 313-345.

[63] Taylor, S.R., McLennan, S.M. The continental crust, its composition and evolution. Blackwell, Oxford 1985; 312 pp.

[64] Pearce, J.A., Bender, J.F., De Long, S.E., Kidd, W.S.F., Low, P.J., Güner, Y., Saroğlu, F., Yılmaz, Y., Moorbath, S., Mıtchell, J.J. Genesis of collision volcanism in eastern Anatolia Turkey. Journal of Volcanology and Geothermal Research 1990; 44: 189-229.

[65] Frey, F.A., Green, D.H., Roy, S.D. Integrated models of basalt petrogenesis: a study of quartz tholeiites to olivine melilitites from South Eastern Australia utilizing geochemical and experimental petrological data. J Petrol 1978; 19: 463-513.

[66] Pearce, J.A. Trace element characteristics of lavas from destructive plate boundaries. In: Thorpe, R.S. (eds) Andesites. Orogenic andesites and related rocks, John Wiley and Sons 1982; 525-548.

[67] Guo, F., Li, H.X., Fan, C.W., Li, J.Y., Zhao, L., Huang, M.W., Xu, W.L. Early Jurassic subduction of the Paleo-Pacific Ocean in NE China: Petrologic and geochemical evidence from the Tumen mafic intrusive complex. Lithos 2015; 224-225: 46-60.

[68] Hofmann, A.W. Chemical differentiation of the earth: The relationship between mantle, continental crust and oceanic crust, Earth and Planetary Science Letters 1988; 90: 297-314.

[69] Smith, E.I., Sanchez, A., Walker, J.D., Wang, K. Geochemistry of mafic magmas in the hurricane volcanic fieid, Utah: Implications for small and large scale chemical variability of the lithospheric mantle, Journal of Geology 1999; 107: 433-448.

[70] Guo, Z., Wilson, M., Liu, J., Mao, Q. Post-collisional, potassic and ultrapotassic magmatism of the northern Tibetan plateau: constraints on characteristics of the mantle source, geodynamic setting and uplift mechanism. Journal of Petrology 2006; 47: 1177-1220.